

Full Length Article

Influence of PbCl₂ and KCl salt mixture on high temperature corrosion of alloy 625Alice Moya Núñez ^{a,*}, Eric Börjesson ^a, Hanna Kinnunen ^b, Daniel Lindberg ^c, Rikard Norling ^a^a Division of Materials and Production, Department of Corrosion, Research Institutes of Sweden, Isafjordsgatan 28A, Kista 16407, Sweden^b Valmet Technologies Oy, Lentokentäkatu 11, Post Office Box 109, FI-33101 Tampere, Finland^c Department of Chemical and Metallurgical Engineering, School of Chemical Engineering, Aalto University, Kemistintie 1F, P.O. Box 16100, FI-00076 Aalto, Finland

ARTICLE INFO

ABSTRACT

Keywords:

High temperature corrosion
Waste-to-energy
Lead chloride
Potassium chloride
Corrosion
Salt mixtures

Aggressive corrosion can occur when firing waste or bio-based fuels, due to the presence of high concentrations of heavy metals, alkali metals, and chlorides. These deleterious compounds deposit on furnace walls and can form mixtures that can rapidly accelerate corrosion. The effect of salts containing lead had not been studied extensively at temperatures lower than 400 °C in nickel-based materials. This study investigates the effect of the individual salts PbCl₂ and KCl and their mixture on the high temperature corrosion of alloy 625 at 340 °C and 380 °C. Samples of alloy 625 were covered with individual salts or a salt mixture and exposed to high temperatures in an atmosphere of synthetic air, 20-vol% H₂O, and 100 ppm HCl. The results show that the presence of individual salts does not induce observable corrosion attack on alloy 625 after 168 h at any tested temperature. The salt mixture did cause a severe corrosion attack at 380 °C, observed after 24 h of exposure. It is suggested that the salt mixture induces the formation of lead chromates that may prevent or disrupt the formation of a protective chromia scale. It is believed that a key part of the mechanism is the formation of eutectic melts by the interaction of the scale with the salt mixture. Thermodynamic equilibria calculations show that the first melting temperature of PbCl₂ and KCl salt mixture after reaction with oxygen can be as low as about 382 °C, and even lower (357 °C) if chromates are present.

1. Introduction

Societal challenges such as climate change due to anthropogenic activities has driven industry to find ways to become less reliant on fossil fuels. Waste and bio-based fuels are becoming widely accepted as a reliable, abundant, and cost-effective alternative to fossil fuels. Despite great advantages, there are many challenges to overcome due to the uncontrolled and heterogenous nature of their compositions. One of the significant issues is the aggressive corrosion that can occur due to high concentrations of deleterious compounds, often present in these alternative fuel forms, containing heavy metals, alkali metals, and chlorides. The effects of corrosion can decrease operational temperatures of waste and biomass fired boilers, as well as lowering their performance by hindering heat transfer.

In an effort to increase steam temperatures in waste-to-energy and biomass boilers, research must be conducted to elucidate complex and often synergistic effects between corrosion products and contaminants.

Heavy metals such as zinc and lead, especially as metal-chlorides, are

known to enhance corrosion at metal temperatures as low as 350 °C [1–6]. The presence of lead found both in field samples and fly ash in waste-to-energy boilers has pushed the research forward in relation to its role in the high temperature degradation of boiler components [6–9]. In particular, salt mixtures containing a combination of PbCl₂ and KCl have been found in field exposures in waste-fired power plants exhibiting melt temperatures in the 400–500 °C range [10]. The effect of lead on low-alloyed steels has been investigated by Talus et al. [11] in a fluidised bed test rig at 350 °C and 400 °C, reporting the formation of a eutectic melt at 400 °C by the reaction of PbCl₂ and KCl salts, accelerating the initial corrosion. Nonetheless, accelerated corrosion was not observed in higher alloyed materials potentially as a result of the formation of a protective chromium-rich oxide. These findings indicate that the corrosion process in low-alloyed steels itself could play an important role in the formation of a low melting eutectic mixture. Later laboratory studies have indicated as well that the mechanism of the eutectic melt formation is affected both by the presence of lead, and by the inherent corrosion process of the affected material [12]. Indeed, the KCl-PbCl₂

* Corresponding author.

E-mail address: alice.moya.nunez@ri.se (A. Moya Núñez).

system in the presence of FeCl_2 has been shown to decrease the solidus temperature of the mixture, experimentally measured to 311 °C for one particular composition [13]. With respect to salt mixtures, Niemi et al. [14] compared the initial corrosivity of mixed and pure salts on carbon steel after 24 h of exposure, concluding that in gradient furnace experiments at 400 °C, pure PbCl_2 shows increased corrosion rate compared to salt mixtures containing PbCl_2 mixed with NaCl or KCl , possibly due to the salt interaction and formation of deposits that bind lead (e.g. K_2PbCl_4). The salt mixture effect at 350 °C in isothermal exposures has been studied by Kinnunen et al. [13], reporting increased oxidation in a low alloyed ferritic steel when PbCl_2 salts were mixed with K_2SO_4 , which was suggested to be caused by the formation of a low melting ternary eutectic involving FeCl_2 . In relation to the corrosivity of pure salts on low-alloyed steel, Larsson et al. [15] have reported increased corrosion after 24 h of exposure at 400 °C with pure KCl salts compared to pure PbCl_2 salts, possibly due to the formation of a eutectic melt in the FeCl_2 - KCl system. It has been reported that at 400 °C pre-oxidized low alloyed ferritic steel degrades faster in the presence of a mixture of PbCl_2 and KCl , compared to pure KCl , suggesting that the formation of PbCrO_4 disrupts a protective oxide layer [16] thus enhancing the corrosion rate. At higher temperatures (500 °C) the reported effect is even more pronounced. Moreover, KCl as an individual salt has been shown to form potassium dichromate ($\text{K}_2\text{Cr}_2\text{O}_7$) when interacting with pure chromium at 650 °C [17] or with 9Cr-1Mo steel at 700 °C [18]. This compound has been observed to form a melt at 375 °C when mixed with KCl [19].

Despite advances in the understanding of the degradation processes, the full mechanism pertaining to the formation of low melting compounds by the interaction of salts and corrosion products remains elusive, particularly for higher alloyed materials. These materials such as alloy 625 have long been used in power boilers due to their superior high temperature corrosion resistance. However, the synergistic effect of lead-based salt mixtures at <400 °C has not been extensively researched for these types of alloys in controlled laboratory studies. Understanding the mechanisms of degradation will facilitate the development of more versatile and longer-lasting materials for boiler applications. Thus, the aim of this study is to determine the corrosivity of lead potassium salt mixes coupled with the influence of temperature on the high temperature corrosion of alloy 625. It has previously been observed that alloy 625 exhibited increased corrosion rates at temperatures close to 380 °C during a field exposure in a combined heat and power (CHP) plant and notably lower rates close to 350 °C, using waste-wood as fuel which had high concentrations of Cl and Pb [20]. Thus, a modest increase in temperature could result in a significant increase in corrosion rate of alloy 625 during specific exposure conditions. The temperatures of the exposures in the present study (340 °C and 380 °C) were chosen based on this observation with the aim of investigating the cause of this behaviour.

2. Materials and methods

TriPLICATE samples of alloy 625 were prepared by cutting coupons (15 × 15 × 4 mm) from a round bar (see Table 1 for elemental composition). Coupons were ground using abrasive silicon carbide paper up to grit size P1200 on all sides and later ultrasonically cleaned in an ethanol bath for 15 min.

Isothermal high temperature exposures were conducted using a horizontal tube furnace (Entech ETF 50/12-III), heated up at a 10 °C/min rate. The furnace temperature was calibrated to within ±3 °C. Before introducing alloy 625 coupons into the furnace at room temperature, a synthetic salt deposit was deposited on top of the samples.

Table 1
Chemical composition of the exposed samples of Alloy 625 (wt%).

Ni	Cr	Fe	Mo	Nb	C	Mn	Si	P	S	Al	Ti	Co	Ta
61.83	20.99	4.00	8.35	3.533	0.015	0.16	0.23	0.01	0.001	0.25	0.31	0.014	0.0167

Each sample was covered with 60 mg/cm² of a salt mixture comprised of 50–50 molar% of PbCl_2 and KCl . The salts were mixed using a mortar and a pestle in solvent-free conditions. Exposures performed with the individual salts were conducted using the same amount of PbCl_2 and KCl as in the salt mixture (47.3 mg/cm² for PbCl_2 and 12.7 mg/cm² for KCl). The atmosphere inside the furnace was composed of synthetic air with 20-vol% H_2O and 100 ppm HCl . The concentrations of H_2O and HCl were selected to simulate relevant levels of these compounds in the flue gas of a waste-to-energy plant [12,21]. Fig. 1 shows a schematic diagram and picture of the exposure set up, including the placement of triplicate samples inside the tube furnace.

The exposure temperatures were 340 °C and 380 °C, and were chosen after consideration of the field exposure in reference [20]. The exposure time was 168 h with the addition of a shorter 24 h exposure for the most severe condition in order to investigate the time dependence of the corrosion attack for that condition. Table 2 summarizes the test matrix.

After exposure, cross sectional samples were prepared by moulding one of the coupons from each exposure into conductive media and grinding them on abrasive SiC paper up to grit size P4000. All exposed specimens were dry ground to avoid unintentionally dissolving Cl containing compounds.

Samples were characterized using a scanning electron microscope SEM (Zeiss Sigma VP 300), equipped with energy dispersive spectroscopy EDS (X-max^N). Investigation via SEM and EDS were conducted in backscatter mode at 20 kV acceleration voltage. The SEM and EDS equipment were controlled through the software SmartSEM (v.5.4) and Aztec (v.6.0) respectively. The EDS results are semi-quantitative in nature and the accuracy depends on the actual conditions of the analysis. The authors estimate that absolute accuracy is between 1 and 2 significant digits. However, for comparison usage of results from same analysis series additional digits are useful. Hence, the data are reported with a higher number of significant numbers. The phases present in unexposed and exposed specimens (not moulded into conductive media) were characterized by X-ray diffraction XRD (Bruker D8 Discover) and the peaks were indexed using the Crystallographic Open Database (COD) [22] and reference [23]. Prior to the XRD measurements, most specimens were tilted about 90° to remove loosely adhering salt from the surface. All XRD-measurements were conducted using a Cu K_α source and a Ni-filter was used to filter out unwanted wavelengths.

3. Calculations

Thermodynamic equilibria calculations were performed using the software FactSage version 8.2 [24], aiming to determine the first melting temperatures of several relevant systems. Liquidus projections of selected ternary (reciprocal) systems were also calculated. The aim of the calculations was to determine if the stable compounds that may form in the studied system (involving interactions between the base alloy, corrosion products, and deposits) could form eutectic melts at or close to the exposure temperatures.

The thermodynamic data for the gas phase and the solid compounds were taken from the Fact Pure Substance database (FactPS), and the data for the molten salt was a custom-made database, based on the FTSalt database. The liquid phase considers the cations K^+ , Pb^{2+} , Cr^{2+} , Cr^{3+} , Fe^{2+} , Fe^{3+} , Ni^{2+} , and the anions Cl^- , CrO_4^{2-} , and O^{2-} . The non-ideal interaction parameters for all chloride binary and higher order systems were taken from the FTSalt database, except for the KCl - CrCl_2 - CrCl_3 system, which was taken from the paper by Ard et al [25]. All other subsystems containing CrCl_2 or CrCl_3 were considered ideal. In addition, the chromate or oxide containing systems were considered

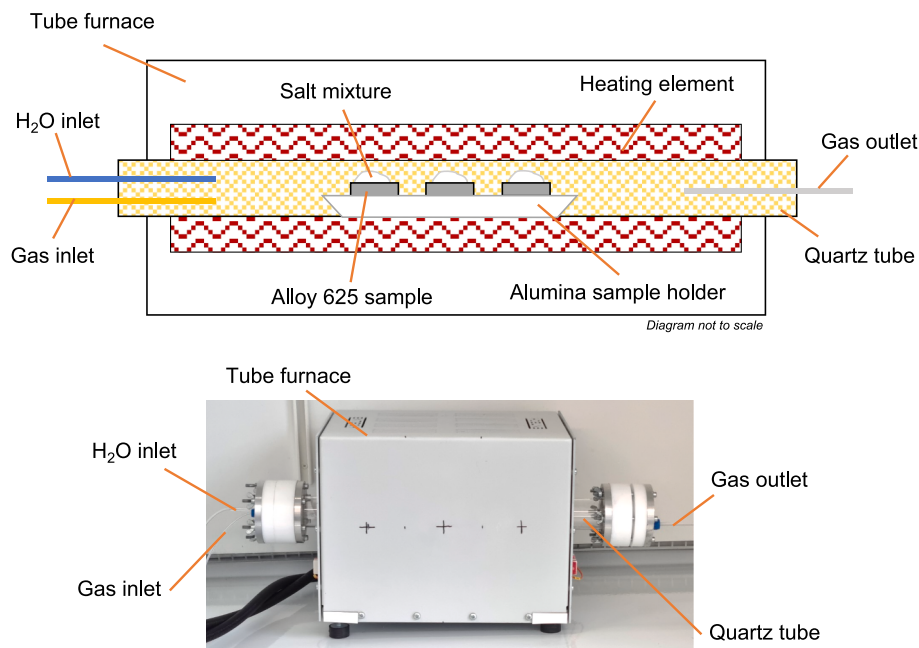


Fig. 1. Schematic diagram (top) and picture (bottom) of the exposure set up, including the placement of triplicate samples inside the tube furnace.

Table 2

Exposure test matrix.

Salt mixture	Temperature [°C]	Duration [h]
PbCl ₂ -KCl	340	168
PbCl ₂ -KCl	380	24
PbCl ₂ -KCl	380	168
PbCl ₂	380	168
KCl	380	168

ideal, including K₂CrO₄-PbCrO₄, PbO-PbCrO₄, and PbCrO₄-PbCl₂. Thermodynamic data for the solid Pb-Cr-O compounds PbCrO₄, Pb₂CrO₅, and Pb₅CrO₈ were taken from the studies of Sahu et al [26–28]. Thermodynamic data for K₂Pb(CrO₄)₂ was estimated based on

the thermodynamic data for K₂Pb(SO₄)₂ by Jin et al. [29] assuming the same ΔH and ΔS from potassium and lead chromates as for the corresponding sulphates. The standard entropy of Pb₂CrO₅ was slightly modified to fit the melting point of the compound to the observed value by Jaeger & Germs (920 °C) [30] and Mal'tsev et al [31].

4. Results

4.1. Deposit/scale analysis

Coupons of alloy 625 were exposed to high temperatures in the presence of pure PbCl₂ and KCl salts, as well as their mixture, aiming to study their influence on the high temperature corrosion of the alloy. The results show that the individual salts did not induce discernible

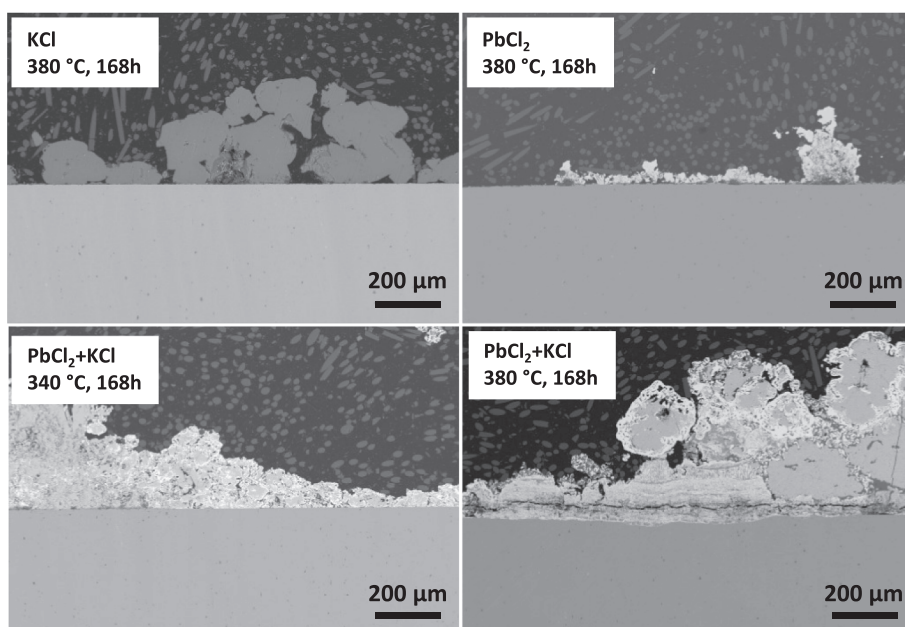


Fig. 2. Overview backscatter SEM-images of cross-section samples exposed at 340 °C or 380 °C for 168 h.

corrosion at 380 °C. Conversely, the salt mixture at the same temperature resulted in a strong corrosion attack on alloy 625, suggesting a synergistic degradation mechanism that involves the effect of both salts in combination. The accelerated corrosion attack was only observed in specimens exposed to the PbCl₂-KCl salt mixture at 380 °C for 24 h and 168 h; at 340 °C however the attack was negligible in comparison (Fig. 2).

As described, the exposures containing individual salts did not induce a severe corrosion attack. Furthermore, oxide layers were not identified by XRD or EDS, nor there was evidence of the formation of compounds from the interaction of the metallic substrate and the salt deposit. Specimens exposed to the PbCl₂-KCl salt mixture at 340 °C showed little to no corrosion after 168 h of exposure; no pits or preferential corrosion zones were identified. XRD analysis of this specimen shows strong peaks corresponding primarily to the base metal, accompanied with a weak indication of other phases that were not identified. Thus, there was no evidence of a significant interaction between the metallic substrate and the salt mixture at this temperature.

The accelerated corrosion attack related to the PbCl₂-KCl salt mixture at 380 °C was observed even after just 24 h of exposure (see Fig. 3) albeit to a lesser degree. After exposure to the PbCl₂-KCl salt mixture, the deposits were analysed, and these were mostly comprised of pure individual salts and two K-Pb-Cl compounds. At the lower temperature, more individual pure salts areas were observed in the cross sections than at the higher temperature. After 24 h of exposure, nearly all the PbCl₂ and KCl have reacted to form KPb₂Cl₅ and K₂PbCl₄, according to EDS analyses. KPb₂Cl₅ was confirmed by XRD analysis (see Table 3 and Fig. 4). However, to the best of our knowledge there are no public databases containing the crystallographic information for the K₂PbCl₄ compound, therefore this compound was not possible to confirm by XRD. After 168 h the K₂PbCl₄-phase is still present according to EDS measurements, but the KPb₂Cl₅-phase is no longer observed. Instead, grains of K₂PbCl₄ are observed surrounded by a phase that has been identified by EDS and XRD as PbCl(OH).

The corrosion attack in the salt mixture exposures was not homogeneous across the surface of the specimens. This was observed in the specimen exposed at 380 °C during 168 h, exhibiting areas where only a small amount of corrosion products had been formed while in others, a rapidly grown oxide had formed protrusions extending up to approximately 500 μm (see Fig. 5).

Features resembling pits were observed in the specimen exposed to the salt mixture at 380 °C during 24 h (see Fig. 6). These pits contained Pb, K and Cl along the metal/oxide-deposit interface. The corrosion products forming on top of these pits consisted of a two-phased layered structure: a Pb-rich phase and a Ni-rich phase. A similar two-phased layered structure of corrosion products having interacted with the salt mixture is observed at the same temperature after 168 h in the PbCl₂-KCl

Table 3

Crystalline compounds detected by XRD and their relative intensity.

Relative intensity	PbCl ₂ – 380 °C – 168 h	KCl – 380 °C – 168 h	PbCl ₂ -KCl – 340 °C – 168 h	PbCl ₂ -KCl – 380 °C – 24 h	PbCl ₂ -KCl – 380 °C – 168 h
Strong	FCC -γ-Ni	FCC -γ-Ni	FCC -γ-Ni	FCC -γ-Ni	FCC -γ-Ni
Medium	KCl			KPb ₂ Cl ₅ *	PbCl(OH)*
				Pb ₄ O ₄ Cl ₂ *	Pb ₂ CrO ₅
				PbCrO ₄	
Weak				NiO	PbMoO ₄
				NiO	

* Compound identified only in non-tilted specimens. Remaining specimens were tilted 90° before the XRD analysis, for the purpose of removing loosely adhering salt.

salt mixture exposure, however exhibiting a coarser morphology with thicker layers (see Fig. 7). No indication of a protective chromia scale is observed in the vicinity of these pits or along the substrate interface. Most of the chromium in the corrosion products is observed in connection with the Pb-rich phase. In the 168 h PbCl₂-KCl salt mixture exposure these pits seemed to have coalesced or widened, giving an indication that the origin of the pits is a key step in the formation and growth of the layered corrosion structure. Moreover, shallow pit-like features were observed throughout most of the heavily corroded areas in this specimen, directly at the metal/oxide-deposit interface. Compositionally these areas are characterized by a slight enrichment of Fe, a depletion of Cr, and the presence of Pb, K and Cl (Fig. 8). Close to the substrate interface, the corrosion products largely resemble the corrosion products observed in the specimen exposed for 24 h.

The chromium-rich layer appearing both after 24 and 168 h of the PbCl₂-KCl salt mixture exposure has been investigated by EDS and XRD. The analyses suggest that this phase contains lead (II) chromate (PbCrO₄) for the 24 h exposure, and lead chromate oxide (Pb₂CrO₅) for the 168 h exposure. The nickel-rich layer is mostly composed of nickel oxide.

4.2. Thermodynamic calculations

The liquidus and solidus projections of several subsystems relevant to the study were calculated. The results for the K₂CrO₄-PbCrO₄-KCl-PbCl₂ system (liquidus & solidus) and K₂O-PbO-KCl-PbCl₂ (only solidus) are shown in Fig. 9 and Fig. 10. The diagrams show that for both systems the first melting temperatures could fall below 390 °C. Other less complex system can also be considered. Table 4 presents the calculated lowest first melting temperature (also known as the solidus temperature) for a number of binary and ternary systems comprised of the salts KCl and PbCl₂ together with their chromates and oxides. All these systems show first melting temperatures above 400 °C. More complex multi-

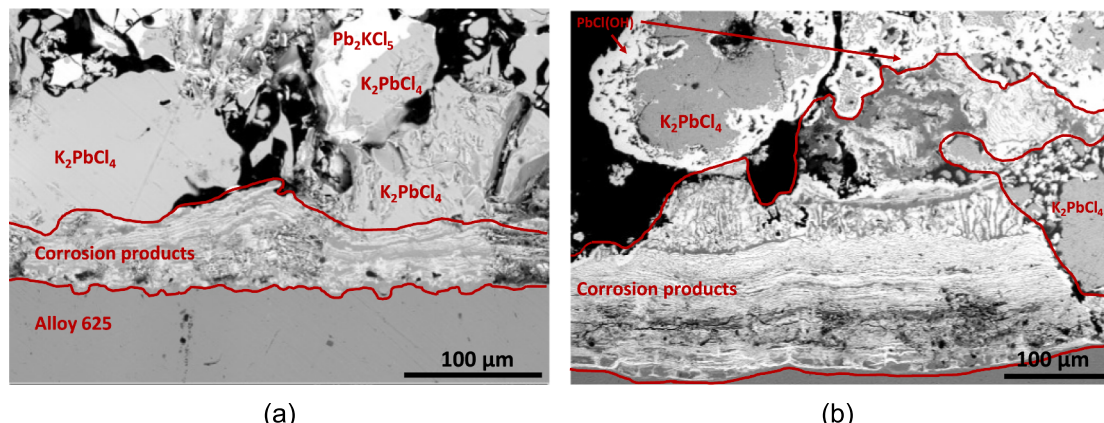


Fig. 3. SEM-images of cross-section samples exposed to the PbCl₂-KCl salt mixture at 380 °C: (a) 24 h of exposure; (b) 168 h of exposure.

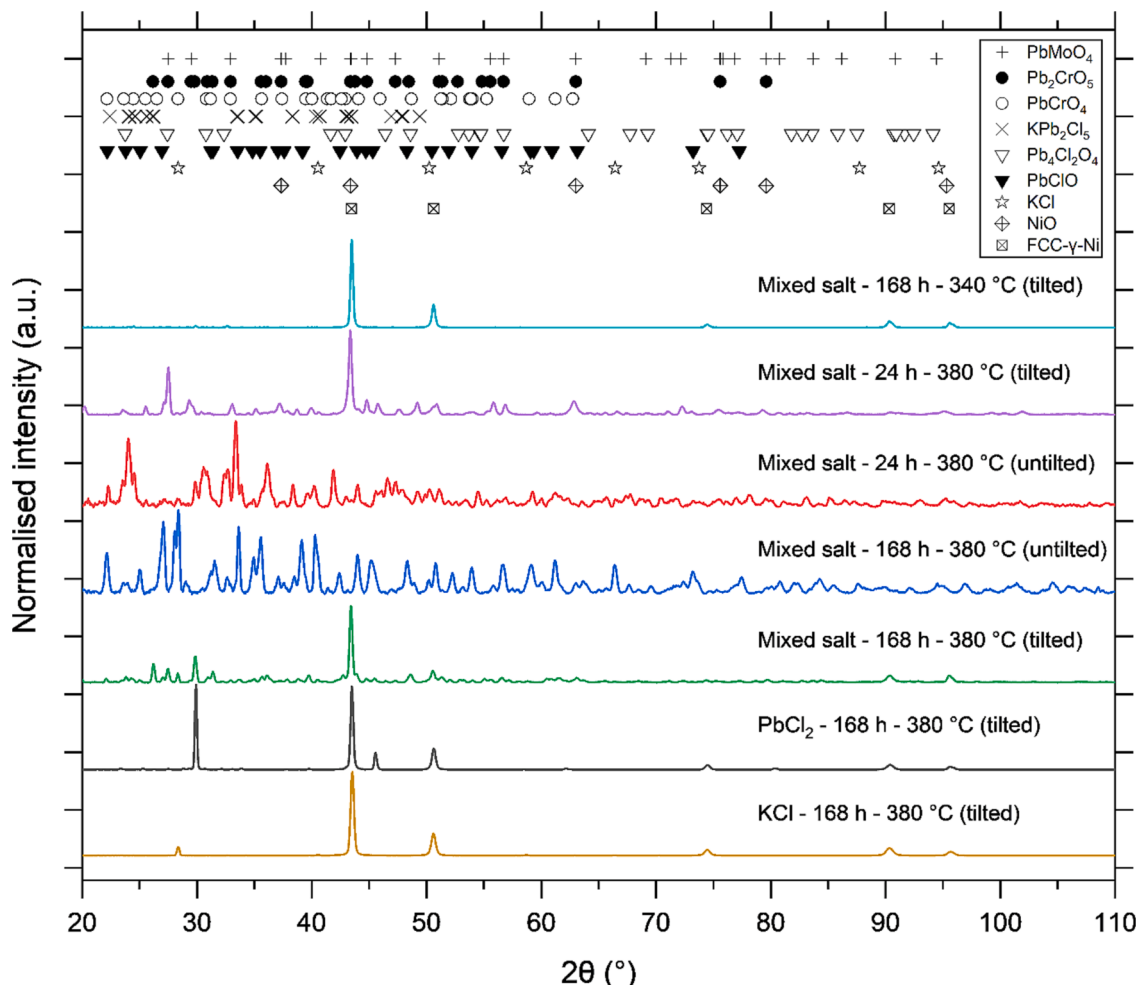


Fig. 4. X-ray diffraction patterns of exposed specimens. X-ray line positions of the identified crystalline compounds are shown at the top of the graph (Crystallographic Open Database (COD) [22]).

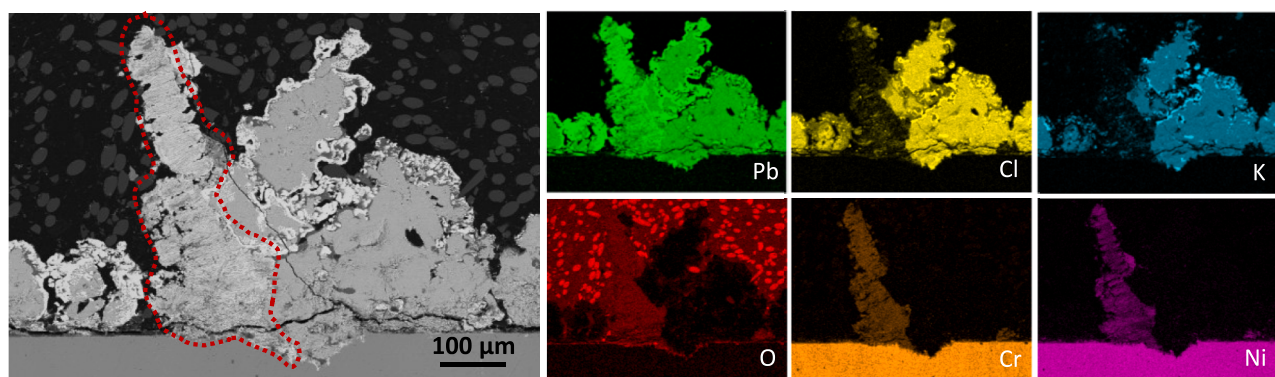


Fig. 5. SEM image (BSD) and corresponding EDS maps of corrosion products on alloy 625, exposed to $\text{PbCl}_2\text{-KCl}$ at 380°C for 168 h. An oxide-containing protrusion spanning nearly 500 μm is encircled in dashed lines. Neighbouring the protrusion, unreacted salt mixture is located on top of a mostly unaffected metal surface.

component systems have also been investigated and are presented in Table 5. These are based on the cationic constituents K, Pb and a selection of the anionic constituents Cl, CrO_4 , O. The systems showing the lowest first melting temperatures of 389°C and 382°C are the same as the ones for which the solidus projections are given in Fig. 9 and Fig. 10, respectively. The multicomponent system containing all the constituents (Pb , K / Cl, CrO_4 , O) resulted in 357°C . Furthermore, the lowest first melting temperature has been calculated for systems comprised of KCl and PbCl_2 together with base metal chlorides that may form originating

from a corroding alloy (Table 6). The system $\text{KCl}\text{-}\text{PbCl}_2\text{-}\text{CrCl}_2$ results in 378°C and $\text{KCl}\text{-}\text{PbCl}_2\text{-}\text{FeCl}_2$ in 312°C .

The phase equilibria as a function of temperature were calculated for different areas in the deposit/oxide layer region to predict melting behaviour and phase equilibria for these compositions.

The results show that parts of the deposit/corrosion product areas (points M1-M3 in Fig. 11 and in Fig. 12 with their corresponding compositions shown in Table 7) can be molten at temperatures below 390°C based on the thermodynamic calculations. The compositions of the

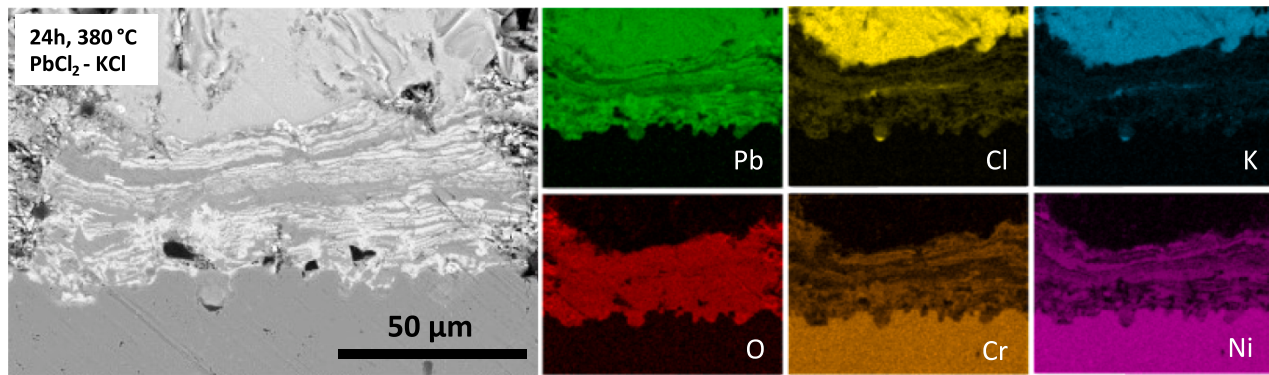


Fig. 6. SEM-image and corresponding elemental maps of corrosion products on alloy 625 exposed to $\text{PbCl}_2\text{-KCl}$ at $380\text{ }^\circ\text{C}$ during 24 h.

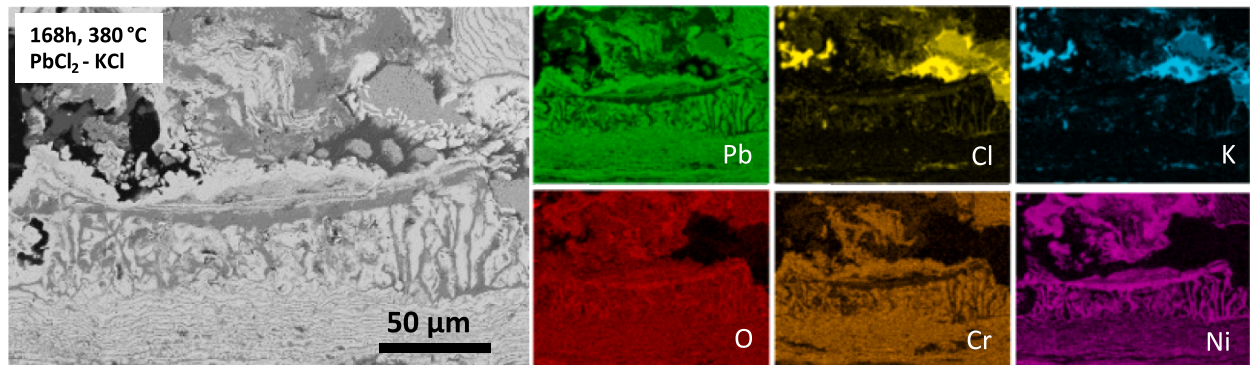


Fig. 7. SEM-image and corresponding elemental maps of corrosion products on alloy 625 exposed to $\text{PbCl}_2\text{-KCl}$ at $380\text{ }^\circ\text{C}$ during 168 h.

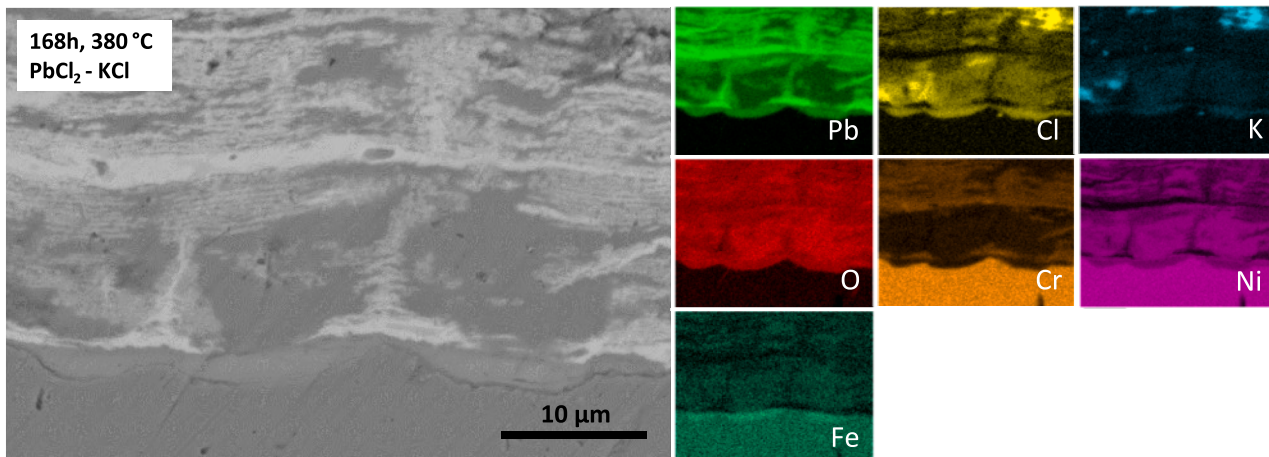


Fig. 8. SEM-image and elemental maps of the substrate interface of alloy 625 exposed to $\text{PbCl}_2\text{-KCl}$ at $380\text{ }^\circ\text{C}$ for 168 h.

deposits/corrosion products at M1 and M2 are approximately equivalent, suggesting that the local area is somewhat homogeneous. The composition at M3 slightly differs, which is also shown by the difference in contrast in the SEM backscatter image. Considering uncertainties in the thermodynamic data, it is not unlikely that for corrosion experiments at $380\text{ }^\circ\text{C}$, the deposit mixtures may have been partially molten.

5. Discussion

The results of this study showed a rapid corrosion attack when exposing alloy 625 to a $\text{PbCl}_2\text{-KCl}$ salt mixture at $380\text{ }^\circ\text{C}$, compared to exposure at $340\text{ }^\circ\text{C}$. At the lower temperature cross sectional analysis did

not reveal corrosion products at the surface of the substrate, while at the higher temperature oxide protrusions were formed extending up to approximately $500\text{ }\mu\text{m}$. The aggressive corrosion attack was only observed when the specimens were exposed to the salt mixture; at $380\text{ }^\circ\text{C}$ the individual salts showed virtually no evidence of corrosion in the examined specimens. The results suggest the formation of a molten phase involving both salts in combination which has induced a significantly higher corrosion attack. The proposed mechanism of degradation in this study is in line with previous studies showing that heavy metals such as lead can decrease the first melting temperature of deposits, which can cause severe corrosion attack in nickel alloys [1,13,32]. However, the formation of a melt is not required for a deposit to induce

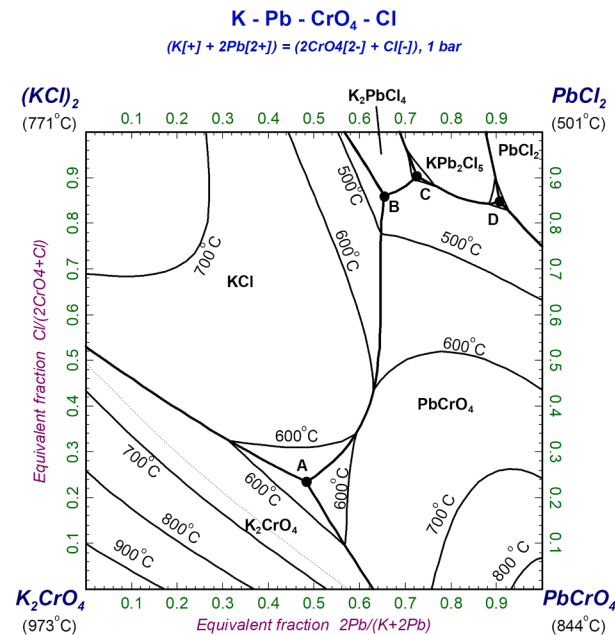
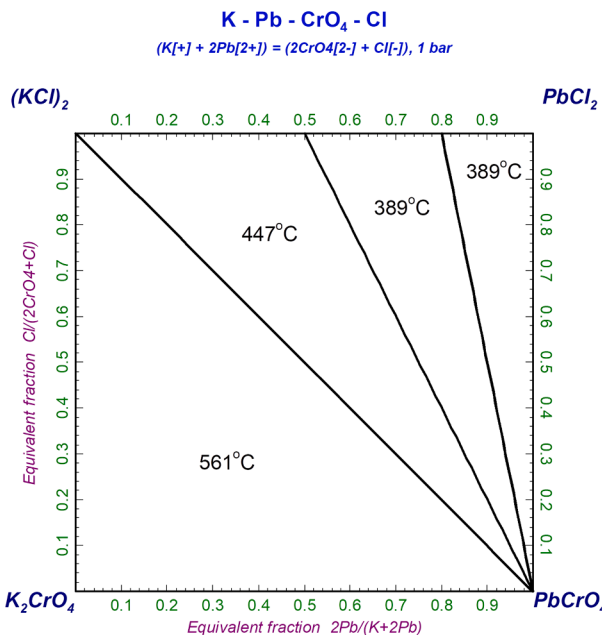


Fig. 9. Solidus (left) and liquidus (right) projections for the $\text{K}_2\text{CrO}_4\text{-PbCrO}_4\text{-KCl}\text{-PbCl}_2$ system. A, B, C and D in the liquidus projection correspond to invariant points in the system. The lowest first melting temperature for the system is about 389 °C.

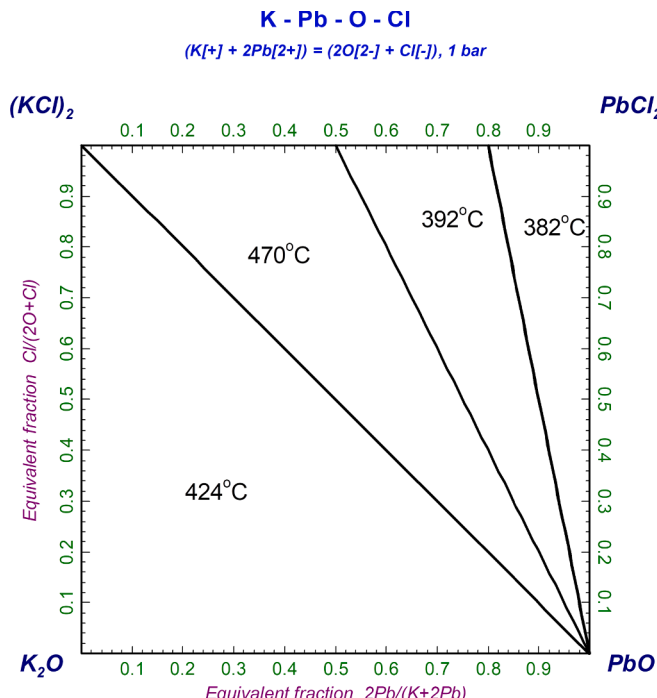


Fig. 10. Solidus projection for the $\text{K}_2\text{O}\text{-PbO}\text{-KCl}\text{-PbCl}_2$ system. The lowest first melting temperature for the system is about 382 °C.

corrosion, which may occur regardless due to the formation of for example volatile metal chlorides [16].

The compounds KPb_2Cl_5 and K_2PbCl_4 were identified either by EDS or XRD analysis, localized on top of the corrosion products after 24 h of exposure. Both compounds have been observed previously by others in similar laboratory exposures [11,12,33], however only KPb_2Cl_5 has been found in heat transfer surfaces in boilers [2]. It has been reported that K_2PbCl_4 may lower the corrosion rate [14], by binding Pb and Cl and forming a product that is not as corrosive as the pure PbCl_2 salt. In the present study these compounds were not identified at 340 °C.

Table 4

Calculated lowest first melting temperatures for some binary and ternary systems.

System	First melting temperature [°C]
$\text{PbCrO}_4\text{-PbO}$	801
$\text{PbCl}_2\text{-PbCrO}_4$	434
$\text{PbCl}_2\text{-PbO}$	422
$\text{PbCl}_2\text{-PbCrO}_4\text{-PbO}$	421
$\text{KCl}\text{-}\text{CrO}_4$	651
$\text{K}_2\text{CrO}_4\text{-K}_2\text{O}$	639
$\text{KCl}\text{-K}_2\text{O}$	426
$\text{KCl}\text{-}\text{CrO}_4\text{-K}_2\text{O}$	423
$\text{K}_2\text{CrO}_4\text{-PbCrO}_4$	640
$\text{K}_2\text{O}\text{-PbO}$	541
$\text{KCl}\text{-PbCl}_2$	408

Table 5

Calculated lowest first melting temperatures for some multi component systems.

System	First melting temperature [°C]
$\text{K, Pb/CrO}_4, \text{O}$	539
K, Pb/Cl, CrO_4	389
K, Pb/Cl, O	382
$\text{K, Pb/Cl, CrO}_4, \text{O}$	357

Table 6

Calculated lowest first melting temperatures for some ternary systems including base metal chlorides.

System	First melting temperature [°C]
$\text{KCl}\text{-PbCl}_2\text{-CrCl}_3$	419
$\text{KCl}\text{-PbCl}_2\text{-NiCl}_2$	395
$\text{KCl}\text{-PbCl}_2\text{-CrCl}_2$	378
$\text{KCl}\text{-PbCl}_2\text{-FeCl}_2$	312

After 168 h of exposure at 380 °C, K_2PbCl_4 was identified in the deposit and surrounded by the halide lead-based compound $\text{PbCl}(\text{OH})$. However, after 24 h at the same temperature, this compound was not

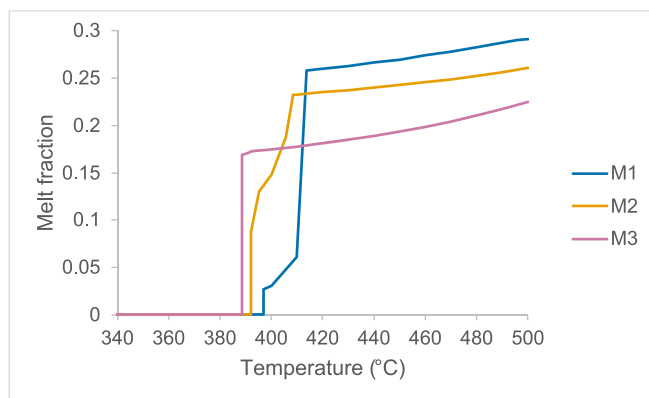


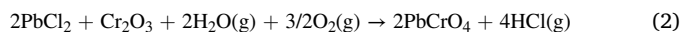
Fig. 11. Melt fraction versus temperature calculated for different areas in the oxide/deposit layer region (M1-M3 points in Fig. 12). The lowest calculated first melting temperature corresponds to point M3 at about 388 °C.

identified. A related lead oxychloride compound ($\text{Pb}_2\text{O}_2\text{Cl}$) has been previously identified in similar laboratory exposures at lower temperatures (340 °C) by Talus et al. on carbon steel specimens [12]. However, no corrosion mechanism involving this compound was suggested in that study. The sole presence of lead oxychlorides in one of the present exposures does not suggest an active role in the initiation of the corrosion mechanism, especially considering it was only identified on the surface of the deposits and not at the metal/scale interface.

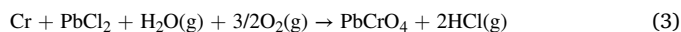
The formation of lead chromates is believed to play an important role in the overall degradation mechanism, as a main cause of chromium consumption and possibly interacting with the salt mixture to form eutectic melts. Indeed, others [3,6,16] have suggested that PbCrO_4 disrupts the formation of protective Cr-containing oxides in stainless steels by the reaction:



Considering the presence of water vapor in the exposure, an alternative reaction involving the formation of lead chromate could be considered:



As chromia was not identified in any exposed specimen, a proposed reaction at 380 °C to form lead chromate from the interaction of lead chloride and chromium may be also the following:



The proposed mechanism involves the formation of a low melting mixture, which can consist of the salt mixture and a potential base metal corrosion product (such as FeCl_2 , CrCl_2 , CrCl_3 , or NiCl_2). Based on the thermodynamic calculations either CrCl_2 or FeCl_2 can form such a melt at the exposure temperature, although the presence of Fe in the alloy is low. It can also be formed by chromate from a corrosion product reacting with the salt mixture together with oxygen, as shown by the multisystem ($\text{Pb}, \text{K}/\text{Cl}, \text{CrO}_4, \text{O}$) equilibrium calculation resulting in a minimum first melting temperature of 357 °C (Table 4).

Considering uncertainties in the thermodynamic data, mixtures that have a calculated first melting temperature somewhat above the exposure temperature are reasonable candidates for melt formation as well. This suggests that reactions by oxygen or chromate alone with the salt mixture can be considered as well. The lowest solidus temperature for a particular composition was calculated to 382 °C (for the $\text{KCl}-\text{PbCl}_2-\text{PbO}-\text{K}_2\text{O}$ system in Fig. 10), and 389 °C for the system containing chromate (Fig. 9).

In connection to the expected melt formation, nickel oxide and lead chromate compounds form in a layered structure. A similar layer-like structure in the scale of alloy 625 has been reported before by Kawahara, albeit at higher temperatures (465 °C metal temperature) after long-term exposure to combustion gas in the presence of boiler deposit [34]. The exposure conditions in this field exposure were harsher than the ones in the current laboratory investigation, inducing for example breakaway corrosion by erosion or changes in local oxidative/reducing conditions, besides the action of molten species. Nonetheless, the similarities in the layered corrosion structure between both investigations may suggest an analogous process involving molten salts as a starting point for a breakaway corrosion event.

The starting point of the aggressive corrosion attack is believed to be pits forming at locations where there was interaction between a possible melt with the base metal. The pits widen in time and more nickel and chromium are diffusing to the deposit/corrosion layer. The corrosion layer grows both towards the deposit and inwards by the widening of the pits. On top, the salt mixture forms $\text{K}-\text{Pb}-\text{Cl}$ compounds that bind lead, potentially inhibiting its diffusion to the surface of the metal and/or evaporation in the tube furnace. The thickness of the observed corrosion

Table 7

Semi-quantitative EDS-point measurements of pits at the interface of alloy 625 exposed to $\text{PbCl}_2 - \text{KCl}$ at 380 °C for 168 h (at%).

Point	O	Cl	K	Cr	Fe	Ni	Nb	Pb
M1	48.15	8.76	1.85	1.72	5.59	24.15	1.99	7.79
M2	47.57	8.41	2.14	2.08	5.12	24.22	2.56	7.9
M3	49.74	5.3	1.63	1.95	1.77	34.12	1.32	4.17

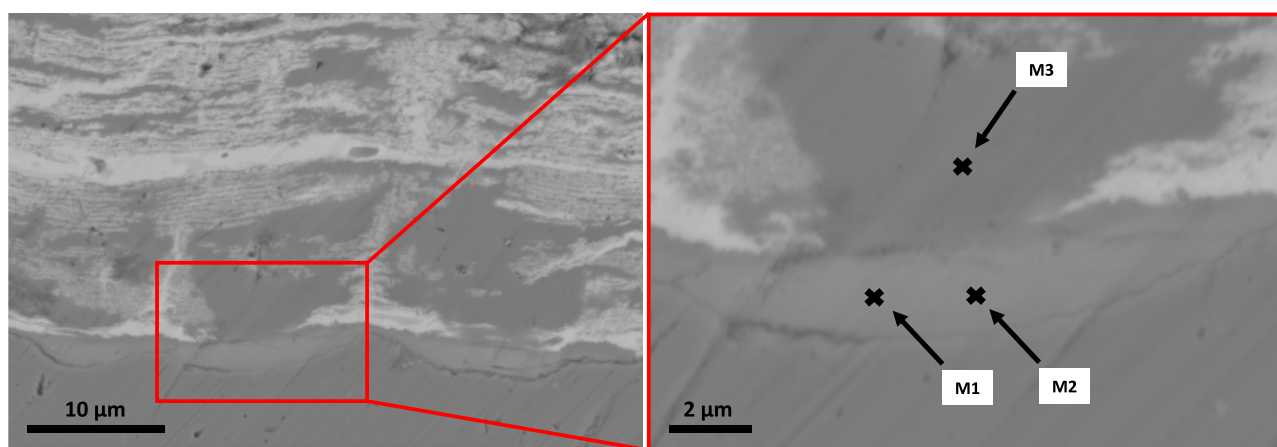


Fig. 12. SEM backscatter images of incipient pits at the substrate interface of alloy 625 exposed to $\text{PbCl}_2 - \text{KCl}$ at 380 °C for 168 h. Right image shows EDS spectra points (M1-M3) from accompanying Table 7.

products after 24 h of exposure is about a third of the thickness after 168 h at the same temperature, suggesting a non-linear scale growth process.

It is believed that the interaction of the salts with each other is key to start the corrosion attack. This is evidenced by the exposures with pure salts, where no corrosion was observed at the same temperature and in the same atmosphere. The first melting temperature of the formed compound is believed to be over 340 °C, as there was no evidence of corrosion attack at this temperature even after 168 h. Equilibria calculations using scale/deposit compositions from the EDS analysis yielded first melting temperatures in the 380–400 °C range (see Fig. 11). The thermodynamic calculations highlight the necessity of the presence of a salt mixture and its interaction with either oxides, chromates, or chlorides to form melts in this temperature range.

Certain aspects of the Hot Corrosion Type II mechanism can be analogous to our proposed mechanism, albeit at higher temperatures (650–800 °C) and in the presence of sulphates. Hot Corrosion in general is defined as the accelerated corrosion at high temperatures from the action of salt species that may form low melting compounds. The corrosion mechanism of Type II has been described as an initial period of pure oxidation followed by the rapid onset of severe corrosion caused by the interaction of the oxidation products with the salt deposit, forming low melting eutectic mixtures that can dissolve the protective oxide films [35–37]. The dissolution mechanism in Type II is non-homogenous therefore leading to localized corrosion attack (pits), which is a feature observed in this study as well.

The dense and uniform appearance of some areas in combination with the layered structure near the pits are proposed to result from at least partially molten phases forming during exposure. Possibly as part of the degradation mechanism, a slight enrichment of Fe was identified in incipient pits in the PbCl₂-KCl exposure at 380 °C, in connection with Cl, O, Pb and K (see Fig. 12 and corresponding Table 7). Indeed, the solidus temperature of the system KCl-PbCl₂-FeCl₂ has been previously measured to 312 °C [13], which may indicate the local formation of melts that could hinder or interfere with a potentially protective chromia layer. However, this iron chloride interaction with the salt mixture cannot explain the full degradation mechanism observed in the current study, as the exposure at 340 °C did not evidence an aggressive corrosion attack. Furthermore, the overall content of Fe in alloy 625 and the iron enrichment itself are both quite modest, which would explain the limited effect of this possible interaction.

The role of other chromates has been reported in literature. The rapid corrosion exhibited by 304-type stainless steel in the presence of KCl at 600 °C has been reported to be caused by the formation of potassium chromate, and the subsequent depletion of Cr leading to a less protective oxide scale [38]. Potassium lead chromate has been confirmed on alloy 625 field specimens, and was attributed to either the disruption of a protective chromia layer or hindering its formation [39]. However, neither potassium chromate nor potassium lead chromate were identified by XRD-analysis in this study, only lead chromate and lead chromate oxide were found.

The full mechanism behind the oxidation of chromium from the bulk to the lead chromates in the corrosion products has not established. Alloy 625 in oxidation conditions at elevated temperatures may form a thin scale composed mainly of Cr₂O₃. The thickness of this layer has been experimentally measured by Auger electron spectroscopy depth profiling to approximately 19 nm when exposed to oxidation conditions at 350 °C [40]. Due to the limited resolution of SEM and EDS such thin layers are extremely challenging to detect. Therefore, it is not established if the PbCl₂-KCl salt mixture breaks down a Cr₂O₃ scale that is continuously formed and consumed, or if the PbCl₂-KCl salt mixture hinders the formation of a Cr₂O₃ scale. The question remains whether alloy 625 is able to form a Cr₂O₃ scale under these conditions, which is rapidly consumed to form PbCrO₄/Pb₂CrO₅, or if Cr from the bulk is directly converted into PbCrO₄/Pb₂CrO₅ without forming Cr₂O₃. Further analysis, for example by transmission electron microscopy, may confirm if there is a Cr₂O₃ layer present.

In short, the discussed considerations taken into account as a whole provide an understanding that the formation of a molten phase is a probable cause of the rapid corrosion attack on alloy 625 at 380 °C during exposure to a PbCl₂ and KCl salt mixture, in contrast to at 340 °C or to the individual salts.

6. Conclusions

Samples of alloy 625 covered with a synthetic salt deposit were exposed to high temperatures in a furnace with an atmosphere composed of synthetic air with 20-vol% H₂O and 100 ppm HCl. Additionally, thermodynamic equilibria calculations were performed to determine the first melting temperatures of several systems. The following conclusions were drawn for the exposure conditions:

- The presence of pure PbCl₂ or KCl salts does not induce any significant corrosion attack on alloy 625 at 380 °C after 168 h of exposure.
- The presence of PbCl₂ and KCl in a 50–50 % molar mixture does not induce any significant corrosion attack on alloy 625 at 340 °C after 168 h.
- The presence of PbCl₂ and KCl in a 50–50 % molar mixture induces a rapid corrosion attack on alloy 625 at 380 °C.
- It is suggested that during exposure to PbCl₂ and KCl salt mixture, the formation of lead chromates (PbCrO₄ after 24 h and Pb₂CrO₅ after 168 h) may prevent the formation of a protective chromia scale, or disrupt it, by consumption of Cr from the bulk and/or interaction of the scale with the salt mixture, forming eutectic melts.
- Thermodynamic calculations show that the first melting temperature for a PbCl₂ and KCl salt mixture after reaction with oxygen can be as low as 382 °C, and even lower if it also contains chromates.
- Thermodynamic calculations show that the first melting temperature for a PbCl₂ and KCl salt mixture in combination with CrCl₂ can be as low as 378 °C, and even lower in combination with FeCl₂.
- Presence of a molten phase in connection to pits is proposed to be a probable key step in the rapid corrosion attack on alloy 625 at 380 °C during exposure to a PbCl₂ and KCl salt mixture.

Funding

This work was carried out within and funded by the High Temperature Corrosion Centre (HTC) at Chalmers University of Technology, with support from the Swedish Energy Agency.

CRediT authorship contribution statement

Alice Moya Núñez: Writing – review & editing, Writing – original draft, Visualization, Investigation. **Eric Börjesson:** Writing – original draft, Investigation. **Hanna Kinnunen:** Writing – review & editing, Conceptualization. **Daniel Lindberg:** Methodology, Investigation. **Rikard Norling:** Writing – review & editing, Supervision, Conceptualization.

Declaration of Competing Interest

The authors declare that they have no known competing financial interests or personal relationships that could have appeared to influence the work reported in this paper.

Data availability

Data will be made available on request.

References

- [1] Bankiewicz D, Yrjas P, Hupa M. High-temperature corrosion of superheater tube materials exposed to zinc salts. *Energy Fuels* 2009;23:3469–74. <https://doi.org/10.1021/ef801012z>.
- [2] Kinnunen H, Hedman M, Lindberg D, Enestam S, Yrjas P. Corrosion in recycled wood combustion—reasons, consequences, and solutions. *Energy Fuels* 2019;33: 5859–66. <https://doi.org/10.1021/acs.energyfuels.8b04168>.
- [3] Bankiewicz D, Enestam S, Yrjas P, Hupa M. Experimental studies of Zn and Pb induced high temperature corrosion of two commercial boiler steels. *Fuel Process Technol* 2013;105:89–97. <https://doi.org/10.1016/j.fuproc.2011.12.017>.
- [4] Montgomery M, Biede O, Larsen OH. Experiences with Inconel 625 in biomass and waste incineration plants. *Mater Sci Forum* 2006;522–523:523–30. <https://doi.org/10.4028/www.scientific.net/MSF.522-523.523>.
- [5] Ruh A, Spiegel M. Thermodynamic and kinetic consideration on the corrosion of Fe, Ni and Cr beneath a molten KCl-ZnCl₂ mixture. *Corros Sci* 2006;48:679–95. <https://doi.org/10.1016/j.corsci.2005.02.015>.
- [6] Spiegel M. Salt melt induced corrosion of metallic materials in waste incineration plants. *Mater Corros* 1999;50:373–93. [https://doi.org/10.1002/\(SICI\)1521-4176\(199907\)50:7<373::AID-MACO373>3.0.CO;2-T](https://doi.org/10.1002/(SICI)1521-4176(199907)50:7<373::AID-MACO373>3.0.CO;2-T).
- [7] Enestam S, Boman C, Niemi J, Boström D, Backman R, Mäkelä K, et al. Occurrence of zinc and lead in aerosols and deposits in the fluidized-bed combustion of recovered waste wood. Part 1: Samples from Boilers. *Energy Fuels* 2011;25: 1396–404. <https://doi.org/10.1021/ef10478n>.
- [8] Pedersen AJ, Frandsen FJ, Ribe C, Astrup T, Thomsen SN, Lundtorp K, et al. A full-scale study on the partitioning of trace elements in municipal solid waste incineration—effects of firing different waste types[†]. *Energy Fuels* 2009;23: 3475–89. <https://doi.org/10.1021/ef801030p>.
- [9] Alipour Y, Talus A, Henderson P, Norling R. The effect of co-firing sewage sludge with used wood on the corrosion of an FeCrAl alloy and a nickel-based alloy in the furnace region. *Fuel Process Technol* 2015;138:805–13. <https://doi.org/10.1016/j.fuproc.2015.07.014>.
- [10] Viklund P, Hjörnede A, Henderson P, Stålenheim A, Pettersson R. Corrosion of superheater materials in a waste-to-energy plant. *Fuel Process Technol* 2013;105: 106–12. <https://doi.org/10.1016/j.fuproc.2011.06.017>.
- [11] Talus A, Norling R, Wickström L, Hjörnede A. Effect of lead content in used wood fuel on furnace wall corrosion of 16Mo3, 304L and alloy 625. *Oxid Met* 2017;87: 813–24. <https://doi.org/10.1007/s11085-017-9727-3>.
- [12] Talus A, Kinnunen H, Norling R, Enestam S. Corrosion of carbon steel underneath a lead/potassium chloride salt mixture. *Mater Corros* 2019;70:1450–60. <https://doi.org/10.1002/maco.201810650>.
- [13] Kinnunen H, Lindberg D, Laurén T, Uusitalo M, Bankiewicz D, Enestam S, et al. High-temperature corrosion due to lead chloride mixtures simulating fireside deposits in boilers firing recycled wood. *Fuel Process Technol* 2017;167:306–13. <https://doi.org/10.1016/j.fuproc.2017.07.017>.
- [14] Niemi J, Kinnunen H, Lindberg D, Enestam S. Interactions of PbCl₂ with alkali salts in ash deposits and effects on boiler corrosion. *Energy Fuels* 2018;32:8519–29. <https://doi.org/10.1021/acs.energyfuels.8b01722>.
- [15] Larsson E, Gruber H, Hellström K, Jonsson T, Liske J, Svensson J-E. A comparative study of the initial corrosion of KCl and PbCl₂ on a low-alloyed steel. *Oxid Met* 2017;87:779–87. <https://doi.org/10.1007/s11085-017-9765-x>.
- [16] Bankiewicz D, Yrjas P, Lindberg D, Hupa M. Determination of the corrosivity of Pb-containing salt mixtures. *Corros Sci* 2013;66:225–32. <https://doi.org/10.1016/j.corsci.2012.09.024>.
- [17] Li YS, Sanchez-Pasten M, Spiegel M. High temperature interaction of pure Cr with KCl. *Mater Sci Forum* 2004;461–464:1047–54. <https://doi.org/10.4028/www.scientific.net/MSF.461-464.1047>.
- [18] Zhang H, Li Y, Wang W, Ma L, Chen L. A Study on Aggressiveness of KCl to Steel Material in High Temperature in Biomass Boilers. *Atlantis Press*; 2015. p. 164–7.
- [19] Lehmusto J, Lindberg D, Yrjas P, Skrifvars B-J, Hupa M. Studies on the partial reactions between potassium chloride and metallic chromium concerning corrosion at elevated temperatures. *Oxid Met* 2012;77:129–48. <https://doi.org/10.1007/s11085-011-9277-z>.
- [20] Talus A, Henderson P, Linder C, Norling R, Davis C. Högtemperaturkorrasjon i returträ-eldade pannor - Rapport 2018: 488. Energiforsk 2018.
- [21] Sorell G. The role of chlorine in high temperature corrosion in waste-to-energy plants. *Mater High Temp* 1997;14:207–20. <https://doi.org/10.1080/09603409.1997.11689546>.
- [22] Vaitkus A, Merkys A, Gražulis S. Validation of the crystallography open database using the crystallographic information framework. *J Appl Cryst* 2021;54:661–72. <https://doi.org/10.1107/S1600576720016532>.
- [23] Schwarz H. Doppelverbindungen vom Typ Me(MeII(XVIO₄)₂ mit der Struktur von Sr₃(PO₄)₂. III. Chromate. *Zeitschrift für anorganische und allgemeine Chemie* 1966;345:230–45. <https://doi.org/10.1002/zaac.19663450503>.
- [24] Bale CW, Béolis E, Chartrand P, Decterov SA, Eriksson G, Gheribi AE, et al. FactSage thermochemical software and databases, 2010–2016. *Calphad* 2016;54: 35–53. <https://doi.org/10.1016/j.calphad.2016.05.002>.
- [25] Ard JC, Schorne-Pinto J, Azizihia M, Yingling JA, Mofrad AM, Johnson KE, et al. Thermodynamic assessments or reassessments of 30 pseudo-binary and -ternary salt systems. *J Chem Thermodyn* 2023;177:106931. <https://doi.org/10.1016/j.jct.2022.106931>.
- [26] Sahu SK, Ganesan R, Gnanasekaran T. Standard molar Gibbs free energy of formation of Pb₅Cr₈O₈(s), Pb₂Cr₅O₅(s), and Pb₅Cr₄O₈(s). *J Chem Thermodyn* 2010; 42:1–7. <https://doi.org/10.1016/j.jct.2009.06.026>.
- [27] Sahu SK, Ganesan R, Srinivasan TG, Gnanasekaran T. The standard molar enthalpies of formation of Pb₂Cr₅O₈(s) and Pb₅Cr₈O₈(s) by acid solution calorimetry. *J Chem Thermodyn* 2011;43:750–3. <https://doi.org/10.1016/j.jct.2010.12.015>.
- [28] Sahu SK, Sahu M, Srinivasa RS, Gnanasekaran T. Determination of heat capacities of Pb₅Cr₄O₈(s), Pb₂Cr₅O₅(s), and Pb₅Cr₈O₈(s). *Monatsh Chem* 2012;143:1207–14. <https://doi.org/10.1007/s00706-012-0756-y>.
- [29] Jin L, Lindberg D, Tsuchiyama Y, Robelin C. A thermodynamic model for high temperature corrosion applications: The (Na₂SO₄ + K₂SO₄ + ZnSO₄ + PbSO₄) system. *Chem Eng Sci* 2022;260:117847. <https://doi.org/10.1016/j.ces.2022.117847>.
- [30] Jaeger FM, Germs III HC. Über die binären Systeme der Sulfate, Chromate, Molybdate und Wolframate des Bleies. *Z Anorg Allg Chem* 1921;119:145–73. <https://doi.org/10.1002/zaac.19211190110>.
- [31] Mal'tsev VT, Bukalova GA, Manakov VM. Equilibrium diagram of the PbCr₄-PbO-PbSiO₃ system. *Russ J Inorg Chem* 1972;17(2):278–80.
- [32] Zahraei EM, Cuevas-Arteaga C, Verhelst D, Alfantazi A. High temperature corrosion of 625 superalloy under iron-zinc-lead oxide/sulfate/chloride salt mixtures. *ECS Trans* 2010;28:171. <https://doi.org/10.1149/1.3496430>.
- [33] Kinnunen H, Hedman M, Engblom M, Lindberg D, Uusitalo M, Enestam S, et al. The influence of flue gas temperature on lead chloride induced high temperature corrosion. *Fuel* 2017;196:241–51. <https://doi.org/10.1016/j.fuel.2017.01.082>.
- [34] Kawahara Y. High temperature corrosion mechanisms and effect of alloying elements for materials used in waste incineration environment. *Corros Sci* 2002;44: 223–45. [https://doi.org/10.1016/S0001-938X\(01\)00058-0](https://doi.org/10.1016/S0001-938X(01)00058-0).
- [35] Stringer J. Hot corrosion of high-temperature alloys. *Annu Rev Mater Sci* 1977;7: 477–509. <https://doi.org/10.1146/annurev.ms.07.080177.002440>.
- [36] Stringer J. High-temperature corrosion of superalloys. *Mater Sci Technol* 1987;3: 482–93. <https://doi.org/10.1080/02670836.1987.11782259>.
- [37] Meier GH. A review of advances in high-temperature corrosion. *Mater Sci Eng A* 1989;120–121:1–11. [https://doi.org/10.1016/0921-5093\(89\)90712-0](https://doi.org/10.1016/0921-5093(89)90712-0).
- [38] Pettersson J, Asteman H, Svensson J-E, Johansson L-G. KCl Induced Corrosion of a 304-type Austenitic Stainless Steel at 600°C. The Role of Potassium Oxid Met 2005; 64:23–41. <https://doi.org/10.1007/s11085-005-5704-3>.
- [39] Alipour Y, Henderson P, Szakálos P. The effect of a nickel alloy coating on the corrosion of furnace wall tubes in a waste wood fired power plant. *Mater Corros* 2014;65:217–25. <https://doi.org/10.1002/maco.201307118>.
- [40] Norling R, Nyblund A. The influence of temperature on oxide-scale formation during erosion-corrosion. *Oxid Met* 2005;63:87–111. <https://doi.org/10.1007/s11085-005-1953-4>.